ORIGINAL RESEARCH

Identifying the Mechanisms and Molecular Targets of Yizhiqingxin Formula on Alzheimer's Disease: Coupling Network Pharmacology with GEO Database

Tingting Zhang [ID][1,2,*]
Linlin Pan[3,*]
Yu Cao[4]
Nanyang Liu[2]
Wei Wei[1,2]
Hao Li [ID][2]

[1]College of First Clinical Medicine, Shandong University of Traditional Chinese Medicine, Jinan, ShanDong Province, People's Republic of China; [2]Department of Geratology, Xiyuan Hospital, China Academy of Chinese Medical Science, Beijing, People's Republic of China; [3]Department of Chinese Medicine Literature and Culture, Shandong University of Traditional Chinese Medicine, Jinan, Shandong, People's Republic of China; [4]Geriatric Laboratory, Xiyuan Hospital, China Academy of Chinese Medical Science, Beijing, People's Republic of China

*These authors contributed equally to this work

Background: Yizhiqingxin formula (YZQX) is a promising formula for the treatment of Alzheimer's disease (AD) with significant clinical effects. Here, we coupled a network pharmacology approach with the Gene Expression Omnibus (GEO) database to illustrate comprehensive mechanisms and screen for molecular targets of YZQX for AD treatment.

Methods: First, active ingredients of YZQX were screened for the Traditional Chinese Medicine Systems Pharmacology (TCMSP) database with the absorption, distribution, metabolism, and excretion (ADME) parameters. Subsequently, putative targets of active ingredients were predicted using the DrugBank database. AD-related targets were retrieved by analyzing published microarray data (accession number GSE5281). Protein–protein interaction (PPI) networks of YZQX putative targets and AD-related targets were constructed visually and merged to identify candidate targets for YZQX against AD using Cytoscape 3.7.2 software. We performed gene ontology (GO) and Kyoto Encyclopedia of Genes and Genomes (KEGG) pathway analysis to further clarify the biological functions of the candidate targets. The gene-pathway network was established to filter for key target genes.

Results: Forty-three active ingredients were identified, and 193 putative target genes were predicted. Seven hundred and ten targets related to AD were screened with |log2 FC| > 1 and $P < 0.05$. Based on the PPI network, 110 target genes of YZQX against AD were identified. Moreover, 32 related pathways including the PI3K-Akt signaling pathway, MAPK signaling pathway, ubiquitin-mediated proteolysis, apoptosis and the NF-kappa B signaling pathway were significantly enriched. In the gene-pathway network, *MAPK1, AKT1, TP53, MDM2, EGFR, RELA, SRC, GRB2, CUL1*, and *MYC* targets are putative core genes for YZQX in AD treatment.

Conclusion: YZQX against AD may exert its neuroprotective effect via the PI3K-Akt signaling pathway, MAPK signaling pathway, and ubiquitin-mediated proteolysis. YZQX may be a promising drug that can be used in the treatment of AD.

Keywords: Yizhiqingxin formula, Alzheimer's disease, network pharmacology, mechanism, molecular target

Correspondence: Hao Li
Department of Geratology, Xiyuan Hospital, China Academy of Chinese Medical Science, Haidian District, Beijing, People's Republic of China
Tel +86 10 6283 5631
Email xyhplihao1965@126.com

Introduction

Alzheimer's disease (AD) is the major cause of dementia globally, affecting 60–80% of patients,[1] which is considered an enormous public health hazard by the World Health Organization.[2] As a slowly progressive neurodegenerative disorder, the clinical characteristic symptoms of AD include memory deficits,

cognitive dysfunction, and inability to perform normal daily living activities in the latter stages. This seems to be mostly associated with extracellular senile plaques (SPs) and intracellular neurofibrillary tangles (NFTs).[3] The pathophysiology of AD is driven by the deposition of different types of amyloid-beta peptide (Aβ) and hyper-phosphorylation of the au protein.[4,5] The Aβ deposition in the brain originates not only from the Aβ component in the brain but also from the periphery.[6] Of note, previous studies have revealed that mutations in presenilin (PSEN) suppressed the activity of γ-secretase and Aβ generation, thereby triggering AD.[7] Moreover, the interactions of Aβ and tau with cytoplasmic and organelle proteins also play a pivotal role in the pathogenesis of AD.[8] Although great progress has been made regarding our understanding of AD pathogenesis and the course of the disease since the first case was reported by Alois Alzheimer in 1907,[9] there are still no pharmacotherapies available to cure or reverse disease progression. Currently, four drugs for the pharmacologic therapy of AD have been approved by the US Food and Drug Administration (FDA): donepezil, rivastigmine, galantamine, and memantine. However, these treatments are often accompanied by side effects and a heavy financial burden.[10]

Recently, the drive for new therapeutic strategies has focused on traditional Chinese medicine (TCM), which is a unique therapeutic modality, and has been practiced clinically by Chinese for thousands of years due to its better clinical efficacy, fewer side effects, and lower resistance. Importantly, TCM has been an effective treatment of neurological diseases and verified in vitro and in vivo.[11] Yizhiqingxin formula (YZQX) is composed of three Chinese medicines, including radix of *Panax ginseng* (Chinese name: Renshen), rhizome of *Coptis chinensis* (Chinese name: Huanglian), and *rhizome of Conioselinum anthriscoides* (Chinese name: Chuanxiong). Data from our previous study suggested that YZQX promoted autophagy by inhibiting the mTOR signaling pathway, thereby improving brain function and decreasing Aβ accumulation in APP/PS1 mice.[12] Moreover, complex diseases and syndromes treated with TCM are controlled via a multi-ingredient, multi-target, and multi-pathway method.[13] Thus, the pharmacological mechanisms and molecular targets of YZQX remain to be adequately studied using innovative approaches.

Network pharmacology has emerged as a powerful and promising tool, which plays a pivotal role in screening the active substances of TCM, revealing potential targets, and

elucidating specific mechanisms.[14] Moreover, the network pharmacology of TCM focuses on a holistic and systematic understanding of a complex network of interrelationships among components, targets, and diseases.[15,16] In particular, the application of network pharmacology in TCM provides researchers a novel opportunity to acquire systematic insights into TCM, which may pave the way to a new direction for the investigation of underlying pharmacological mechanisms and safety assessment of TCM. In addition, the transcription profile characteristics might unprecedentedly change along with the innovations in microarray technologies and public microarray data repository establishment.[17,18]

Hence, in the present study, we coupled a network pharmacology approach with the Gene Expression Omnibus database (GEO) to further illustrate comprehensive mechanisms, explore underlying pathways, and screen for molecular targets of YZQX for the treatment of AD. First, we screened for active ingredients of YZQX and predicted their putative targets through the search of related databases. Differentially expressed genes (DEGs) between AD and healthy individuals were identified by analyzing microarray data from the GEO database. We identified core networks and targets through the protein–protein interaction (PPI) network method. Moreover, by gene ontology (GO) and pathway analysis, the molecular mechanisms of action of YZQX were clarified. The study flowchart is presented in Figure 1.

Methods
Screening of Active Ingredients in YZQX

All chemical ingredients in YZQX were manually acquired from the Traditional Chinese Medicine Systems Pharmacology (TCMSP) Database (http://tcmspw.com/tcmsp.php),[19] which serves as a unique systematic pharmacology platform to study TCM. The absorption, distribution, metabolism, and excretion (ADME) model[20] was used to predict the pharmacokinetic properties of chemical ingredients. In this process, we employed two vital parameters among all ADME-related properties, including oral bioavailability (OB) and drug-likeness (DL), to identify bioactive ingredients of YZQX. OB represents the efficiency of bioactive ingredients reaching the systemic circulation.[21] DL is a qualitative indicator applied in drug design to estimate the resemblance between an ingredient and a certified drug structure.[22] In our study, our

Step 1 Data sources

TCMSP → Chuanxiong Huanglian Renshen

GEO database GSE5281

Step 2 Identification of targets of Yizhiqingxin formula and Alzheimer's disease

Compound-Target network

DEGs

Step 3 Establishment and analysis of PPI networks

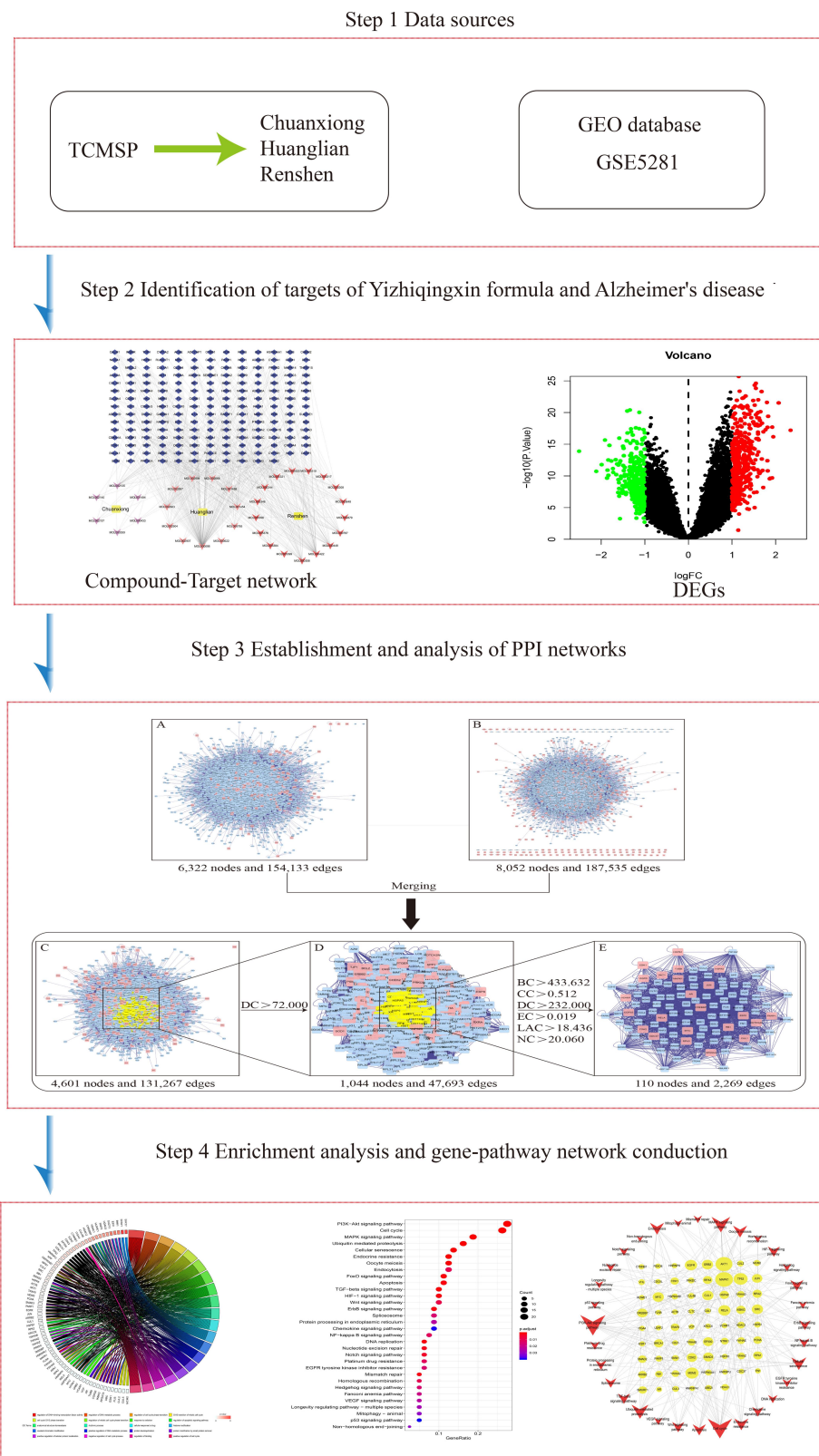Step 4 Enrichment analysis and gene-pathway network conduction

Figure 1 Workflow for Yizhiqingxin formula treatment of Alzheimer's disease.

threshold criteria of OB and DL were greater than 30% and 0.18, respectively.

Identification of Potential Targets

Identification of putative targets of YZQX chemical compounds was performed with DrugBank (https://www.drug bank.ca/),[23] which is a web platform that combines detailed medicine data with abundant drug target information. First, we input all active ingredients into DrugBank to acquire all targets for each ingredient. Then, with species limited to "Homo sapiens", the UniProt database (https://www.uniprot.org/) was used to convert proteins into genes. Eventually, all putative targets of YZQX were retrieved after removing duplicated targets. In addition, we used Cytoscape 3.7.2 software to establish and visualize the compound-target network of YZQX based on the obtained results.

Differentially Expressed Gene Search, Identification, and Analysis

Expression profiling data from GSE5281 were downloaded from the GEO database (http://www.ncbi.nlm.nih.gov/geo/) based on the microarray platform GPL570 (Affymetrix Human Gene Expression Array), which contained 74 samples from healthy individuals and 87 AD samples. Based on the annotation information in the platform, probe IDs were used to identify the corresponding genes. DEGs between patients with AD and healthy individuals were screened using the package limma of R software according to $P < 0.05$, and $|\log2$ fold change $(FC)| > 1$ and were visualized using a volcano plot.

Protein–Protein Interaction Network Construction

The PPI networks of YZQX putative targets and AD-related DEGs were established and visualized using the BisoGenet[24] plug-in of Cytoscape 3.7.2. In this process, two PPI networks were built according to the available PPI databases from the Biomolecular Interaction Network Database (BIND), Biological General Repository for Interaction Datasets (BioGRID), Database of Interacting Proteins (DIP), Human Protein Reference Database (HPRD), IntAct Molecular Interaction Database (IntAct), and Molecular INTeraction Database (MINT).

Network Merge and Analysis

A merged network was thereafter constructed according to the overlapping data from the two PPI networks built earlier. The network topological features of nodes in the merged interaction network were calculated and analyzed using Cytoscape 3.7.2 software plug-in CytoNCA[25] using the following six crucial topological parameters: betweenness centrality (BC), closeness centrality (CC), degree centrality (DC), eigenvector centrality (EC), local average connectivity-based method (LAC), and network centrality (NC). BC is defined as the total number of shortest paths through a node. If the number of shortest paths passing through a node is larger, then intermediary centrality is higher.[26] CC is a measure of the mean distance from a node to other nodes, reflecting the degree of closeness of one node to other nodes.[25] DC refers to the number of links to one node, which reflects the interaction frequency of one node with adjacent nodes.[27] EC calculates the centrality for a node relative to the centrality of its neighbors, which is proportional to the sum of the centrality scores of neighboring nodes.[28] LAC represents the mean local connectivity of its neighbors, which could be used to determine a protein's significance.[29] NC measures a node's significance according to the number of edges it connects and the clustering coefficients of the edges.[30]

First, the degree of centrality was calculated. Notably, if the degree of centrality of a node was more than twice the median degree of centrality of all nodes in a network, the gene that corresponds to that node served as "a big hub" in the network.[31] According to this topological indicator, the network was further extracted for the ensuing analysis. Subsequently, to maximize the screening of key genes in the network, we adopted the corresponding median values of other indicators as the threshold values of the hub nodes in the network analysis. Eventually, a core subnetwork was created based on the above indicators, where these hub genes were considered to have more nodes to transmit information and higher node information transmission efficiency.

GO and KEGG Pathway Analysis of the Core Network

We employed the GO and KEGG pathway analysis to further clarify the biological interpretations of hub genes in the core network. For gene classification and enrichment analyses, clusterProfiler,[32] a new ontology-based package of R version 3.6.0 software, was applied to improve

Table 1 The Final Selected Ingredients in YZQX for Analysis

Drug	Molecular ID	Molecular Name	OB (%)	DL
Chuanxiong	MOL001494	Mandenol	42	0.19
	MOL002135	Myricanone	40.6	0.51
	MOL002140	Perlolyrine	65.95	0.27
	MOL002151	Senkyunone	47.66	0.24
	MOL002157	Wallichilide	42.31	0.71
	MOL000359	Sitosterol	36.91	0.75
	MOL000433	FA	68.96	0.71
Huanglian	MOL001454	Berberine	36.86	0.78
	MOL013352	Obacunone	43.29	0.77
	MOL002894	Berberrubine	35.74	0.73
	MOL002897	Epiberberine	43.09	0.78
	MOL002903	(R)-Canadine	55.37	0.77
	MOL002904	Berlambine	36.68	0.82
	MOL002907	Corchoroside A_qt	104.95	0.78
	MOL000622	Magnograndiolide	63.71	0.19
	MOL000762	Palmidin A	35.36	0.65
	MOL000785	Palmatine	64.6	0.65
	MOL000098	Quercetin	46.43	0.28
	MOL001458	Coptisine	30.67	0.86
	MOL002668	Worenine	45.83	0.87
	MOL008647	Moupinamide	86.71	0.26
Renshen	MOL002879	Diop	43.59	0.39
	MOL000449	Stigmasterol	43.83	0.76
	MOL000358	Beta-sitosterol	36.91	0.75
	MOL003648	Inermin	65.83	0.54
	MOL000422	Kaempferol	41.88	0.24
	MOL004492	Chrysanthemaxanthin	38.72	0.58
	MOL005308	Aposiopolamine	66.65	0.22
	MOL005314	Celabenzine	101.88	0.49
	MOL005317	Deoxyharringtonine	39.27	0.81
	MOL005318	Dianthramine	40.45	0.2
	MOL005320	Arachidonate	45.57	0.2
	MOL005321	Frutinone A	65.9	0.34
	MOL005344	Ginsenoside rh2	36.32	0.56
	MOL005348	Ginsenoside-Rh4_qt	31.11	0.78
	MOL005356	Girinimbin	61.22	0.31
	MOL005357	Gomisin B	31.99	0.83
	MOL005360	Malkangunin	57.71	0.63
	MOL005376	Panaxadiol	33.09	0.79
	MOL005384	Suchilactone	57.52	0.56
	MOL005399	Alexandrin_qt	36.91	0.75
	MOL005401	Ginsenoside Rg5_qt	39.56	0.79
	MOL000787	Fumarine	59.26	0.83

Abbreviations: OB, oral bioavailability; DL, drug-likeness.

understanding of higher-order functions of the biological system. GO consists of three parts: biological process (BP), molecular function (MF), and cellular component (CC). Of note, in both the GO or KEGG functional categories, false discovery rate (FDR) <0.05 was considered significant.
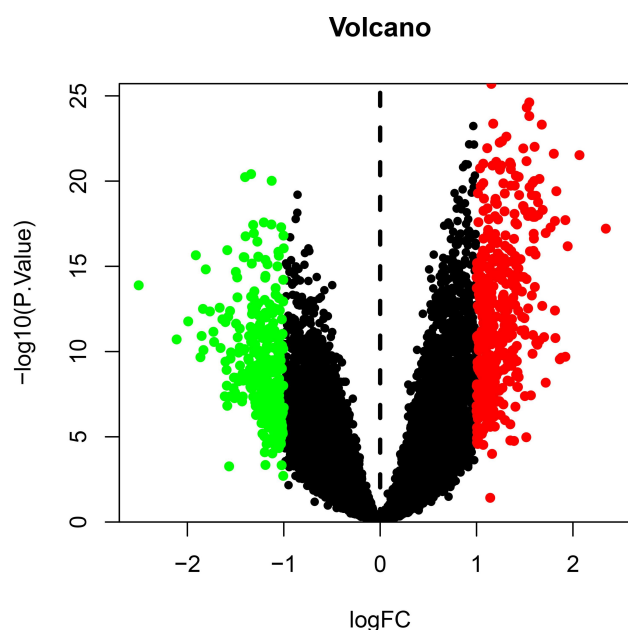

Figure 2 Volcano plot of differentially expressed genes. The red dots represent significantly up-regulated genes, the green dots represent significantly down-regulated genes.

The top 20 terms of GO analysis were selected and further presented visually using the package GOplot in R version 3.6.0 software. In addition, a bubble plot was used to present KEGG enrichment analysis with color-coding: the smaller the *P*-value is in red, and the larger the *P*-value is in blue. The sizes of the dots represent the gene ratio. In addition, we constructed a gene-KEGG pathway network using Cytoscape version 3.7.2 software.

Results
Screening of Bioactive Ingredients and Putative Targets from YZQX

After applying the criteria of OB ≥ 30% and DL ≥ 0.18, all bioactive ingredients of Chinese herbs in YZQX were identified in the TCMSP database. There were 43 bioactive ingredients from filtered YZQX, including 7 in Chuanxiong, 14 in Huanglian, and 22 in Renshen. The chemical ingredients of these Chinese herbs did not overlap with each other. Eventually, all 43 candidate ingredients were chosen for further investigation. The drug names, molecular names, and ADME-related parameters of these compounds are listed in Table 1. The top five ingredients of OB were Corchoroside A_qt (OB = 104.95%), Celabenzine (OB = 101.88%), Moupinamide (OB = 86.71%), FA (OB = 68.96%), and
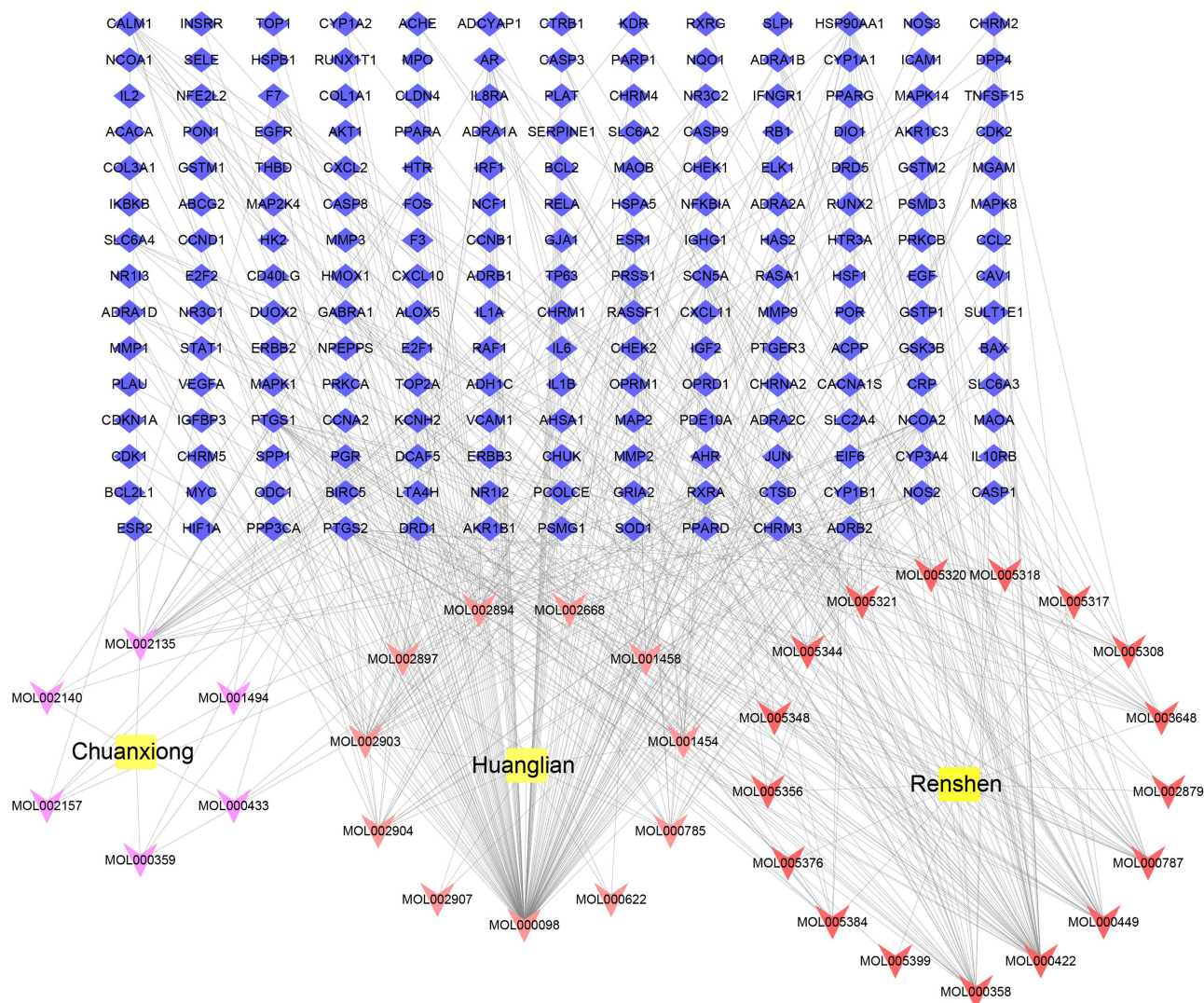
Figure 3 Compound- target network of YZQX. Blue Diamonds represent targets contained in YZQX, yellow squares represent Chinese Herbs, purple vs represent ingredients of Chuanxiong, light red vs represent ingredients of Huanglian, and red vs represent ingredients of Renshen.

Aposiopolamine (OB = 66.65%). The top five DL components included worenine (DL = 0.87), coptisine (DL = 0.86), fumarine (DL = 0.83), gomisin B (DL = 0.83), and berlambine (DL = 0.82).

According to the target screening of the bioactive ingredients in the DrugBank database, a total of 505 target genes in 3 Chinese herbs in YZQX were found, of which, there were 39 targets in Chuanxiong, 251 targets in Huanglian, and 214 targets in Renshen. After removing duplicate targets, 193 potential target genes were selected for the 43 ingredients of YZQX. Moreover, the UniProt database was used to translate the official names of potential targets so that they could be used in network construction for further biological characterization. Detailed information is presented in Table S1.

Identification of AD-Related DEGs

Differential genetic analysis between AD and healthy individuals was performed with $|\log_2 FC| > 1$ and $P < 0.05$. Ultimately, 710 DEGs were identified. A volcano plot of the distribution of DEGs is shown in Figure 2; among them, 415 up-regulated genes are represented by red dots, and 295 down-regulated genes are represented by green dots.

Construction of a Compound-Putative Target Network of YZQX

Chinese herbal compounds can interfere with diseases by regulating a network through binding multiple targets. Therefore, a network, compound-target, was established
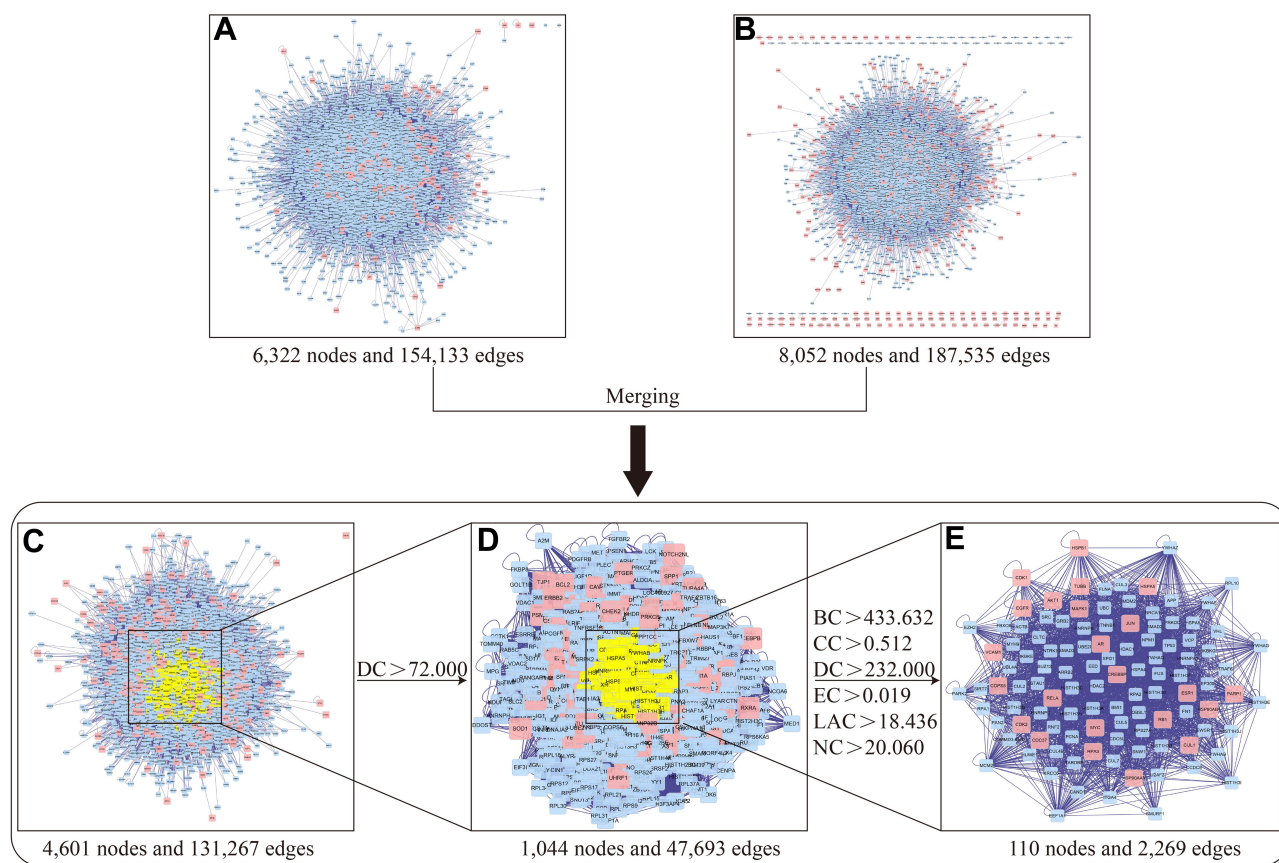
Figure 4 Identification of core targets of YZQX against AD. (**A**) YZQX putative targets PPI network. (**B**) AD-related targets PPI network. (**C**) The interactive PPI network of YZQX putative targets and AD-related targets. (**D**) PPI network of significant proteins extracted from C. (**E**) PPI network of candidate YZQX targets for AD treatment extracted from D.

Abbreviations: AD, Alzheimer's disease; DC, degree centrality; BC, betweenness centrality; CC, closeness centrality; EC, eigenvector centrality; LAC, local average connectivity-based method; NC, network centrality.

to predict these targets through the acquisition of detailed information on the bioactive ingredients of YZQX. This network consisted of 230 nodes and 538 edges (Figure 3), indicating the interactions of chemical compounds and putative targets.

PPI Network Construction, Merging, and Analysis

PPI network analysis contributes to the in-depth understanding of the molecular mechanism of diseases from a systematic perspective and quantifies the function of specific proteins.[33] Hence, we visually constructed PPI networks of YZQX putative targets (Figure 4A), which contained 6322 nodes and 154 133 edges. The PPI network constructed for AD-related targets specifically consisted of 8052 nodes and 187 535 edges (Figure 4B). In the PPI network, nodes and edges represent interacting proteins and interactions, respectively.

Ultimately, these two PPI networks were merged to identify the candidate targets for YZQX against AD, which helped to clarify the underlying mechanism of action of YZQX in AD. The results demonstrated that the YZQX-interacting PPI network comprised 4601 nodes and 131,267 edges in total (Figure 4C). Subsequently, the topological properties of the aforementioned merged PPI network were analyzed according to six key parameters: BC, CC, DC, EC, LAC, and NC, screened targets above two-fold median values of DC as well as more than median values of BC, CC, EC, LAC, and NC as hub genes, thereby establishing the core network of the AD-treated effect of YZQX. Since the median degree of all nodes was 36, the cutoff value of the first screening was DC >72, and the results were cast on 1044 nodes and 47,693 edges (Figure 4D). Subsequently, these 1044 vital targets were screened. The second cutoff values were BC > 433.632, CC > 0.512, DC > 232.000, EC > 0.019, LAC > 18.436, and

Table 2 The Key Parameter Values of 110 Core Targets

Genes	Betweenness	Closeness	Degree	Eigenvector	LAC	Network
NTRK1	34,826.18	0.664755	1289	0.116813	53.29151	277.6773
CUL3	21,198.02	0.635588	826	0.114035	56.47758	229.5985
APP	10,243.13	0.566848	806	0.055436	28.96356	72.53909
HSP90AA1	9460.703	0.576881	767	0.067672	43.58423	114.5966
EGFR	9542.414	0.570569	744	0.053291	33.77992	95.67655
TP53	19,385.39	0.613891	705	0.093969	51.64691	187.0632
ESR1	15,416	0.601847	688	0.088586	47.31073	153.2738
XPO1	9759.544	0.57182	687	0.062664	34.92015	89.52947
MCM2	14,459.25	0.613169	651	0.104016	55.49354	184.1087
HSP90AB1	7073.427	0.567774	640	0.064062	40.888	93.63328
FN1	12,720.53	0.607809	635	0.097986	47.78167	159.2176
CDK2	13,079.84	0.59977	622	0.090112	45.10315	142.7661
UBC	12,601.12	0.585626	614	0.071026	43.33876	131.519
COPS5	8276.179	0.592951	613	0.094499	54.41768	148.6378
CUL1	8951.929	0.593288	564	0.094188	55.54103	152.807
CUL7	9990.143	0.599425	552	0.089742	43.08069	136.2477
RNF2	9862.539	0.584641	525	0.074703	37.84158	110.2017
CAND1	6260.668	0.582682	508	0.090651	58.54333	146.2511
MYC	5971.691	0.55985	503	0.048495	29.34222	67.73357
SIRT7	6146.117	0.569013	496	0.067372	34.51938	80.48613
OBSL1	6856.922	0.584314	489	0.078196	38.68543	108.4209
YWHAZ	7172.03	0.576243	473	0.075107	50.46931	118.5144
NPM1	8227.16	0.588268	469	0.096871	65.23567	160.9559
ITGA4	7832.164	0.586944	466	0.085024	44.23226	116.7656
GRB2	5536.105	0.555674	463	0.051024	35.73333	73.91536
VCP	6197.81	0.563479	440	0.061805	40.44492	85.07729
CDC5L	4925.157	0.562264	423	0.060454	40.74786	86.73088
EP300	6009.564	0.562567	421	0.052032	41.77682	97.50255
VCAM1	6003.134	0.579444	420	0.079334	39.46341	97.94946
CCDC8	5004.908	0.56654	420	0.065573	33.0081	72.19039
FBXO6	4267.925	0.559549	405	0.058117	27.9417	57.70662
HNRNPU	5872.296	0.574339	400	0.08583	63	138.3799
BRCA1	6517.061	0.561054	396	0.049457	31.98253	75.49951
SNW1	6051.717	0.561961	396	0.05577	37.17672	82.74052
HSPA5	5837.462	0.565618	396	0.067442	44.8642	93.19859
TRAF6	6651.395	0.555674	392	0.041215	24.94762	59.68665
EED	4392.456	0.567465	388	0.070736	42.96016	93.1871
HDAC1	3202.844	0.549526	386	0.043028	39.17277	74.42252
HUWE1	6899.481	0.571507	381	0.067745	39.42424	95.38087
EWSR1	4716.752	0.552729	381	0.05213	32.06965	61.19216
HNRNPA1	3161.637	0.559549	376	0.070618	55.08036	99.03541
RPA1	4112.825	0.555082	374	0.056751	36.0566	68.20034
HSPA8	4735.245	0.560451	354	0.060211	41.54425	81.78843
UBE2I	4251.229	0.548082	353	0.040825	27.41304	52.01266
VHL	4526.61	0.553609	353	0.054592	29.57971	54.42804
CUL2	3517.477	0.561054	352	0.068893	40.7193	76.78246
RPA2	3277.309	0.550686	352	0.051589	30.05181	52.91248
YWHAQ	4217.219	0.552729	345	0.052153	33.845	61.33131
MDM2	5224.652	0.553316	344	0.048166	30.26108	59.62867
PARK2	5674.771	0.559549	342	0.053931	29.9417	66.59044
HIST1H3F	2098.438	0.556861	339	0.058623	48.64055	92.1532

(Continued)

Table 2 (Continued).

Genes	Betweenness	Closeness	Degree	Eigenvector	LAC	Network
HIST1H3A	2098.438	0.556861	339	0.058623	48.64055	92.1532
HIST1H3D	2098.438	0.556861	339	0.058623	48.64055	92.1532
HIST1H3G	2098.438	0.556861	339	0.058623	48.64055	92.1532
HIST1H3C	2098.438	0.556861	339	0.058623	48.64055	92.1532
HIST1H3I	2098.438	0.556861	339	0.058623	48.64055	92.1532
HIST1H3J	2098.438	0.556861	339	0.058623	48.64055	92.1532
HIST1H3E	2098.438	0.556861	339	0.058623	48.64055	92.1532
HIST1H3B	2098.438	0.556861	339	0.058623	48.64055	92.1532
HIST1H3H	2098.438	0.556861	339	0.058623	48.64055	92.1532
HDAC5	4650.054	0.565618	332	0.066067	37.55328	78.84761
EEF1A1	4669.956	0.560753	329	0.070422	47.2467	84.56732
HSPB1	2002.872	0.533777	327	0.037852	28.41007	38.56029
CREBBP	2243.336	0.539018	326	0.034659	36.86875	62.29731
CUL5	2082.417	0.551852	323	0.064059	43.43655	68.27214
RPA3	2151.833	0.543796	314	0.04598	29.25882	45.84844
U2AF2	3871.685	0.558052	310	0.05925	43.12844	86.10159
IKBKG	2045.93	0.536799	306	0.035822	27.27211	40.40291
YWHAG	2690.41	0.543512	303	0.045769	34.15476	53.60628
PAN2	3382.067	0.554787	302	0.062376	34.43333	60.47694
AR	3134.942	0.540415	300	0.031188	27.61146	48.51884
SRC	2442.609	0.534598	299	0.025456	25.61029	43.73683
SMURF1	3391.445	0.546646	296	0.045905	24.20556	41.60122
YWHAE	2110.936	0.542382	296	0.050186	38.06024	54.26133
IKBKE	2788.819	0.539855	294	0.03488	18.56962	31.93874
CTNNB1	4842.84	0.547507	291	0.039217	25.30939	49.85884
SUZ12	3175.214	0.548947	290	0.046405	31.03627	56.67218
AKT1	2149.736	0.534598	278	0.028894	23.78832	34.81879
FUS	2869.735	0.553022	277	0.061692	43.76119	71.4498
ARRB2	3047.877	0.54837	270	0.052508	29.98421	50.1614
MAPK1	1661.102	0.530249	267	0.027795	25.20472	36.14141
HSPA4	2869.613	0.5421	267	0.041526	28.74691	45.89033
RELA	2373.639	0.535421	265	0.030975	26.1049	40.14754
STAU1	2901.346	0.551268	265	0.057269	36.70408	61.5319
CUL4B	1886.888	0.542946	258	0.053202	38.61078	54.05284
BMI1	1681.993	0.535146	256	0.033908	23.49645	33.33627
SMAD2	1860.082	0.529442	256	0.025645	20.41322	29.0253
COMMD3-BMI1	1681.993	0.535146	256	0.033908	23.49645	33.33627
PARP1	2103.137	0.53874	256	0.046043	36.66879	50.39636
SMAD3	1986.411	0.533231	255	0.027245	25.03053	38.00191
YWHAB	1680.029	0.530519	255	0.031926	26.15079	35.30965
TARDBP	1933.812	0.545788	253	0.061576	49.70811	74.31153
RPS27A	3022.78	0.543512	253	0.051495	37.50867	55.10979
CLTC	2194.827	0.536523	250	0.039743	28.63265	44.31083
MYH9	1763.332	0.533504	250	0.03501	29.61029	45.29088
TUBB	2383.363	0.544363	249	0.04812	32.77457	50.91263
EZH2	1941.901	0.536799	248	0.040164	30.76471	43.82032
JUN	1296.69	0.527834	247	0.023482	25.16522	34.51743
FLNA	2329.567	0.537352	247	0.0397	31.22819	50.12443
RB1	1898.756	0.53133	246	0.027173	25.60769	37.52534
CDK1	1528.586	0.530789	245	0.033329	26.04724	35.02188

(*Continued*)

Table 2 (Continued).

Genes	Betweenness	Closeness	Degree	Eigenvector	LAC	Network
HDAC2	1782.979	0.536523	244	0.038497	36.54967	54.55134
UBL4A	2439.333	0.544079	244	0.054326	40.25434	56.65844
CDC37	1191.997	0.525441	244	0.026047	22.14019	28.04657
ACTB	2757.472	0.540975	243	0.041952	29.14465	44.85049
RPL10	1536.133	0.537075	243	0.054545	59.01935	75.56065
HNRNPK	2495.745	0.547219	239	0.057228	43.24862	65.25151
XRCC6	1638.875	0.535421	234	0.04306	30.7972	41.1287
PCNA	1721.649	0.531871	234	0.036312	26.9771	36.49264
PRKDC	2304.506	0.540135	233	0.046236	31.32298	45.2468

NC > 20.060. As a result, the second extracted network consisted of 110 nodes and 2269 edges (Figure 4E), which was a core network for YZQX against AD. When the 110 nodes were sorted in descending order presented in Table 2, NTRK1 (degree = 1289), CUL3 (degree = 826), APP (degree = 806), HSP90AA1 (degree = 767), EGFR (degree = 744), TP53 (degree = 705), ESR1 (degree = 688), XPO1 (degree = 687), MCM2 (degree = 651), and HSP90AB1 (degree = 640) were the major hub nodes in the core network.

Enrichment Analysis of the Core Network

To further evaluate the 110 candidate targets, enrichment analysis was performed using the package clusterProfiler in R. The results of GO enrichment analysis demonstrated that 110 genes of the core network were significantly enriched in 1640 GO terms (FDR < 0.05), including 1383 in BP, 121 in CC, and 136 in MF. Detailed information on GO analysis is presented in Table S2. Moreover, the top 20 terms are presented in Figure 5. The results indicated that the most representative GO terms included the regulation of DNA-binding transcription factor activity, regulation of cell cycle phase transition, negative regulation of cell cycle process, positive regulation of cell cycle, regulation of apoptotic signaling pathway, nuclear chromatin, transcription factor complex, protein-DNA complex, ubiquitin ligase complex, ubiquitin-protein ligase binding, ubiquitin-like protein ligase binding, cell adhesion molecule binding, DNA-binding transcription activator activity, RNA polymerase II-specific, ubiquitin-like protein transferase activity, and activating transcription factor binding, which suggested the well-documented

biological effects on cell proliferation, ubiquitin-proteasome system, and apoptosis.

In addition, a total of 32 related pathways according to the KEGG analysis were identified (FDR < 0.05) (Figure 6), mainly including the PI3K-Akt signaling pathway, Cell cycle, Cellular senescence, MAPK signaling pathway, ubiquitin-mediated proteolysis, apoptosis and NF-kappa B signaling pathway, and p53 signaling pathway.

Gene-Pathway Network Analysis

Based on the analysis of KEGG by clusterProfiler of R, a gene-pathway network was established with the aforementioned signal pathways and the corresponding target genes, which are displayed in Figure 7. This gene-pathway network showed interactions in multiple pathways involving cross-talk of the transitive relationship between the pathway terms and genes. A total of 102 nodes and 247 edges were found in the gene-pathway network. The topological analysis of 32 pathways and 70 genes was calculated with a certain degree. According to Figure 7, it was preliminarily speculated that the above ingredients of YZQX could be used for the treatment of AD via the PI3K-Akt signaling pathway, cell cycle, MAPK signaling pathway, ubiquitin-mediated proteolysis, and cellular senescence due to the high representation of *MAPK1, AKT1, TP53, MDM2, EGFR, RELA, SRC, GRB2, CUL1*, and *MYC* targets.

Discussion

AD is an age-related heterogeneous disease, while effective treatments remain scarce. YZQX is a promising formula for the treatment of AD in TCM clinical practice with significant clinical effects, which has been demonstrated in previous studies.[12,33] Hence, this study
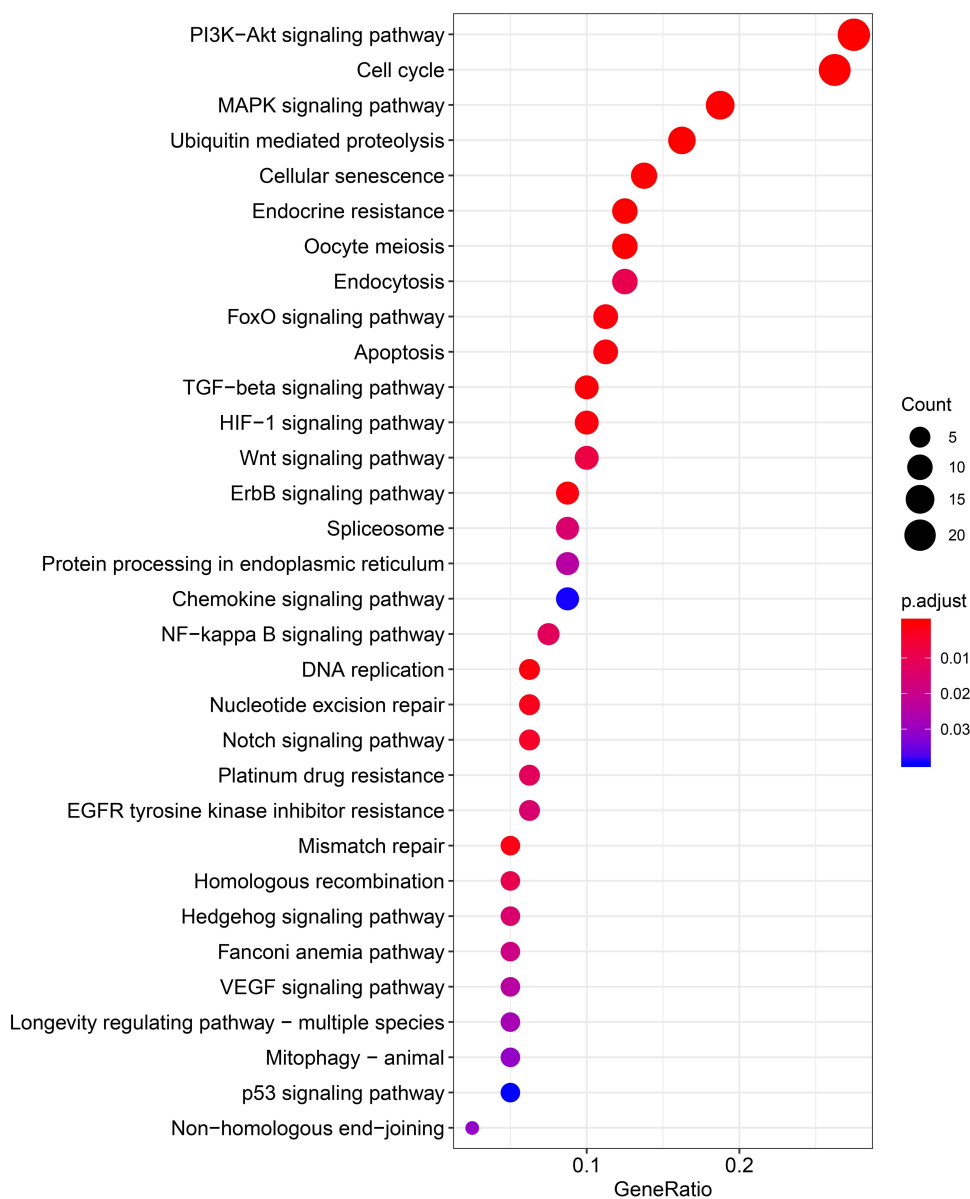
Figure 5 Go analysis of core targets. (**A**) Biological process; (**B**) Cellular component; (**C**) Molecular function.
Notes: Chord plot displays the relationship between genes and terms.

performed a comprehensive analysis of network pharmacology coupled with gene expression profiling to further identify the underlying mechanisms and therapeutic targets of YZQX in AD. The findings identified 110 key target genes, 33 related signal pathways, and 43 chemical compounds for YZQX in the treatment of patients with AD. By constructing the gene-KEGG network, 10 common genes including *MAPK1, AKT1, TP53, MDM2, RELA, EGFR, SRC, MYC, GRB2*, and *CUL1*, were considered as key target genes of YZQX treating AD.

A compound-target network of YZQX was generated in the present study, which demonstrated that the majority of compounds affected multiple targets; for example, quercetin, kaempferol, beta-sitosterol, stigmasterol, fumarine, (R)-canadine, and myricanone acted on 141, 56, 28, 27, 27, 26, and 23 targets, respectively. Moreover, the majority of YZQX compounds may have overlapping targets, which provided a synergistic effect, suggesting that YZQX acts in a multi-component and multi-target way. Quercetin is a natural flavonoid often found in fruits and vegetables and has anti-inflammatory, antioxidant, and neuroprotective effects.[34,35] The long-term preventive administration of quercetin led to a meaningful improvement in the development of histopathological features and cognitive dysfunction in triple transgenic mouse models of AD.[36] A growing body of evidence demonstrates that quercetin may contribute to neuroprotective actions against AD mainly through inhibiting the aggregation of Aβ, the formation of NFTs, β-site amyloid precursor protein (APP)-cleaving enzyme 1 (BACE1), acetylcholinesterase (AChE), and others.[37] Importantly, the neuroprotective effects of quercetin are primarily associated with MAPK signaling cascades and PI3K/Akt pathways.[37] Kaempferol is also a flavonoid, which is abundant in multiple types of foods and beverages, such as tea, broccoli, apples, strawberries, and beans,[38] with antioxidant, anti-inflammatory, and neuroprotective properties.[39,40] The neuroprotective effects of kaempferol were mediated via regulating the protein expression levels of Bcl-2, apoptosis-inducing factor (AIF), and mitogen-activated protein kinase (MAPK).[40] Beta-Sitosterol is one of the most extensively distributed plant sterols, with a structure similar to cholesterol.[41] Studies performed on dietary plant sterols suggested that it could accumulate in the brain through the blood-brain barrier, thereby potentially affecting brain function.[42] Moreover, beta-Sitosterol can change the shear mode of amyloid precursor protein (APP),[43] as well as prevent the deposition of Aβ and

Figure 6 KEGG pathway enrichment of core targets of YZQX against AD. Pathways that had significant changes of p.adjust <0.05 were identified. The dot size represents number of genes and color represents p.adjust value.

enhance the improvement of cognitive dysfunction in APP/PS1 mice.[44] The pathogenesis of AD is complicated, and it is widely accepted that neurodegeneration can be triggered by a series of interactions including inflammation, oxidative stress, and apoptotic cell death.[45–47] In the present study, due to their antioxidant, anti-inflammatory, and neuroprotective properties, quercetin, kaempferol, and beta-sitosterol may be key compounds for YZQX.

In addition, a PPI network of YZQX against AD was screened with 110 nodes and 2269 edges, thus highlighting a potential role in AD. YZQX probably exerts therapeutic effects on AD by regulating these particular core targets. Furthermore, we performed functional enrichment analysis of these core protein targets and found that the mechanisms of YZQX against AD were closely related to the following pathways: (1) PI3K-Akt signaling pathway, (2) MAPK signaling pathway, (3) ubiquitin-mediated proteolysis, (4) cell cycle, cellular senescence, apoptosis, (5) Wnt signaling pathway, (6) ErbB signaling pathway, and (7) NF-κB signaling pathway. Many signaling pathways have been associated with AD. The PI3K-Akt signaling pathway participates in various cell functions such as autophagy, cell survival, protein synthesis, and
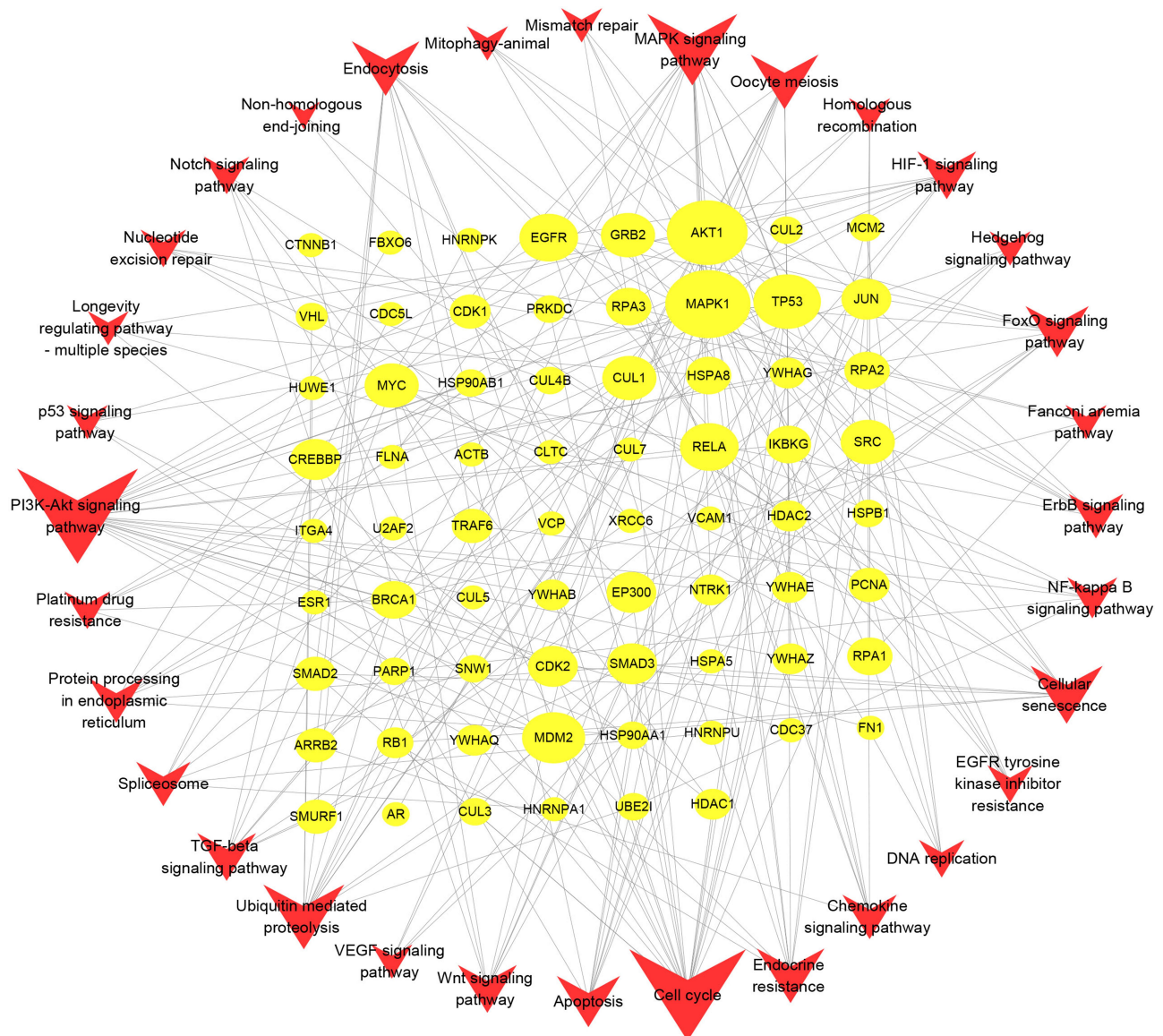
Figure 7 Gene-Pathway Network. The topological analysis of 32 pathways and 70 genes was calculated with the degree. The yellow circles represent target genes and the red vs represent pathways. Big size represents the larger degree.

glycolysis. Furthermore, Akt is also a key survival-promoting factor that inhibits apoptotic signaling. The PI3K/Akt/mTOR signaling pathway modulates autophagy and clears protein aggregates during neurodegeneration.[48] When it was over-activated, the level of neuronal autophagy was inhibited and clearance of intracellular Aβ and tau was delayed, which also aggravated the production of amyloid plaques and NFTs of the AD brain to a certain extent.[49] The MAPK signaling pathway is one of the classic inflammation pathways, composed of JNK, ERK, and p38. Studies have suggested that the activated MAPK pathway may be involved in the pathogenesis of AD via the following mechanisms: induction of neuronal apoptosis[50–53] as well as transcription and enzymatic activation

of β- and γ-secretases.[54,55] Moreover, Schnöder et al found that in an AD mouse model, inhibiting neuronal p38-MAPK enhanced autophagy and promoted BACE1 degradation, thereby reducing Aβ generation in neurons and Aβ load in the brain.[56] Moreover, as a eukaryotic cell intracellular major protein degradation system, mounting evidence has implicated ubiquitin-mediated proteolysis in the pathogenesis of AD.[57,58] Ubiquitin can bind to proteins and label them for degradation; for example, it can bind to APP and γ-secretase activated protein, which are associated with the etiology of AD.[59,60] Accordingly, in principle, some of the symptoms of AD were ameliorated by modulating the function of the ubiquitin-proteasome pathway components.[61] Consequently, YZQX

may be neuroprotective through related signaling pathways in the process of AD treatment.

To reveal key targets of YZQX against AD in the related pathways, we also constructed a gene-pathway network. The results demonstrated that *MAPK1* showed the maximum degree and therefore, it may be considered as the core target gene. In addition to *MAPK1*, other core target genes including *AKT1, TP53, MDM2, RELA, EGFR*, and *MYC* obtained from this network, elicit a very potent vital effect on the process of YZQX against AD. As a natural negative regulatory factor of MAPKs, *MAPK1* plays a significant role in the dephosphorylation of MAPKs.[62] Evidence provided by Meng et al revealed that *MDM2* is a vital information transmitter that activates AKT and suppresses p53-induced cell apoptosis.[63]

In summary, we adopted a network pharmacology approach to elucidate the underlying molecular mechanisms and target genes of YZQX against AD in the present study. Quercetin, kaempferol, and beta-Sitosterol, which regulate most of the targets, may be considered as key compounds of YZQX. Furthermore, YZQX may exert its regulatory function via the following pathways: PI3K-Akt signaling pathway, MAPK signaling pathway, and ubiquitin-mediated proteolysis. *MAPK1, AKT1, TP53, MDM2, RELA, EGFR*, and *MYC* were the core targets in the gene-pathway network of YZQX against AD. YZQX and its components may be promising drugs that can be used to treat AD.

Author Contributions

All authors made a significant contribution to the work reported, whether that is in the conception, study design, execution, acquisition of data, analysis and interpretation, or in all these areas; took part in drafting, revising or critically reviewing the article; gave final approval of the version to be published; have agreed on the journal to which the article has been submitted; and agree to be accountable for all aspects of the work.

Funding

Disclosure

The authors report no conflicts of interest in this work.

References

1. Mebane-Sims I. 2020 Alzheimer's disease facts and figures. *Alzheimers Dement*. 2020.
2. Lane CA, Hardy J, Schott JM. Alzheimer's disease. *Eur J Neurol*. 2018;25(1):59–70. doi:10.1111/ene.13439
3. Solanki I, Parihar P, Parihar MS. Neurodegenerative diseases: from available treatments to prospective herbal therapy. *Neurochem Int*. 2016;95:100–108. doi:10.1016/j.neuint.2015.11.001
4. Majd S, Power JH, Grantham HJ. Neuronal response in Alzheimer's and Parkinson's disease: the effect of toxic proteins on intracellular pathways. *BMC Neurosci*. 2015;16(69).
5. Morris M, Maeda S, Vossel K, Mucke L. The many faces of tau. *Neuron*. 2011;70(3):410–426. doi:10.1016/j.neuron.2011.04.009
6. Uddin MS, Kabir MT, Tewari D, et al. Revisiting the role of brain and peripheral Aβ in the pathogenesis of Alzheimer's disease. *J Neurol Sci*. 2020;416:116974. doi:10.1016/j.jns.2020.116974
7. Kabir MT, Uddin MS, Setu JR, et al. Exploring the role of PSEN mutations in the pathogenesis of Alzheimer's disease. *Neurotox Res*. 2020.
8. Uddin MS, Al Mamun A, Rahman MA, et al. Emerging proof of protein misfolding and interaction in multifactorial Alzheimer's disease. *Curr Top Med Chem*. 2020;20. doi:10.2174/1568026620666200601161703
9. Alzheimer A. Uber eine eigenartige Erkrankung der Hirnride. *Centralblatt Nervenheilkunde Psychiatr*. 1907;30:177–179.
10. Patterson C. World Alzheimer report 2018. The state of the art of dementia research: new frontiers. An analysis of prevalence, incidence, cost and trends. *Alzheimers Dis Int*. 2018.
11. Ong WY, Farooqui T, Koh HL, Farooqui AA, Ling EA. Protective effects of ginseng on neurological disorders. *Front Aging Neurosci*. 2015;7:129.
12. Yang Y, Wang Z, Cao Y, et al. Yizhiqingxin formula alleviates cognitive deficits and enhances autophagy via mTOR signaling pathway modulation in early onset alzheimer's disease mice. *Front Pharmacol*. 2019;10:1041. doi:10.3389/fphar.2019.01041
13. Liu X, Wu J, Zhang D, Wang K, Duan X, Zhang X. A network pharmacology approach to uncover the multiple mechanisms of hedyotis diffusa willd. on colorectal cancer. *Evid Based Complement Alternat Med*. 2018;2018:6517034. doi:10.1155/2018/7802639
14. Hopkins AL. Network pharmacology. *Nat Biotechnol*. 2007;25(10):1110–1111. doi:10.1038/nbt1007-1110
15. Cao H, Li S, Xie R. Exploring the mechanism of dangguiliuhuang decoction against hepatic fibrosis by network pharmacology and experimental validation. *Front Pharmacol*. 2018;9:187. doi:10.3389/fphar.2018.00187
16. Huang T, Ning Z, Hu D. Uncovering the mechanisms of chinese herbal medicine (mazirenwan) for functional constipation by focused network pharmacology approach. *Front Pharmacol*. 2018;9:270. doi:10.3389/fphar.2018.00270
17. Butte A. The use and analysis of microarray data. *Nat Rev Drug Discov*. 2002;1(12):951–960.
18. Lu Y, Huggins P, Bar-Joseph Z. Cross species analysis of microarray expression data. *Bioinformatics*. 2009;25(12):1476–1483. doi:10.1093/bioinformatics/btp247
19. Ru J, Li P, Wang J, et al. TCMSP: a database of systems pharmacology for drug discovery from herbal medicines. *J Cheminform*. 2014;6(1):13. doi:10.1186/1758-2946-6-13
20. Barton HA, Pastoor TP, Baetcke K, et al. The acquisition and application of absorption, distribution, metabolism, and excretion (ADME) data in agricultural chemical safety assessments. *Crit Rev Toxicol*. 2006;36(1):9–35. doi:10.1080/10408440500534362
21. Xu X, Zhang W, Huang C, et al. A novel chemometric method for the prediction of human oral bioavailability. *Int J Mol Sci*. 2012;13(6):6964–6982. doi:10.3390/ijms13066964

22. Tao W, Xu X, Wang X, et al. Network pharmacology-based prediction of the active ingredients and potential targets of Chinese herbal Radix Curcumae formula for application to cardiovascular disease. *J Ethnopharmacol*. 2013;145(1):1–10. doi:10.1016/j.jep.2012.09.051

23. Law V, Knox C, Djoumbou Y, et al. DrugBank 4.0: shedding new light on drug metabolism. *Nucleic Acids Res*. 2014;42 (Databaseissue):D1091–1097. doi:10.1093/nar/gkt1068

24. Martin A, Ochagavia ME, Rabasa LC, Miranda J, Fernandez-de-Cossio J, Bringas R. BisoGenet: a new tool for gene network building, visualization and analysis. *BMC Bioinform*. 2010;11(1):91. doi:10.1186/1471-2105-11-91

25. Tang Y, Li M, Wang J, Pan Y, Wu FX. CytoNCA: a cytoscape plugin for centrality analysis and evaluation of protein interaction networks. *BioSystems*. 2015;127:67–72. doi:10.1016/j.biosystems.2014.11.005

26. Newman MEJ. A measure of betweenness centrality based on random walks. *Soc Networks*. 2005;27(1):39–54. doi:10.1016/j.socnet.2004.11.009

27. Jeong H, Mason SP, Barabási AL, Oltvai ZN. Lethality and centrality in protein networks. *Nature*. 2001;411(6833):41–42. doi:10.1038/35075138

28. Bonacich P. Power and centrality: a family of measures. *Am J Sociol*. 1987;92(5):1170–1182. doi:10.1086/228631

29. Li M, Wang J, Chen X, Wang H, Pan Y. A local average connectivity-based method for identifying essential proteins from the network level. *Comput Biol Chem*. 2011;35(3):143–150. doi:10.1016/j.compbiolchem.2011.04.002

30. Wang J, Li M, Wang H, Pan Y. Identification of essential proteins based on edge clustering coefficient. *IEEE/ACM Trans Comput Biol Bioinform*. 2012;9(4):1070–1080. doi:10.1109/TCBB.2011.147

31. Li S, Zhang ZQ, Wu LJ, Zhang XG, Li YD, Wang YY. Understanding ZHENG in traditional Chinese medicine in the context of neuro-endocrine-immune network. *IET Syst Biol*. 2007;1 (1):51–60. doi:10.1049/iet-syb:20060032

32. Yu G, Wang LG, Han Y, He QY. clusterProfiler: an R package for comparing biological themes among gene clusters. *OMICS*. 2012;16 (5):284–287. doi:10.1089/omi.2011.0118

33. Wang F, Feng J, Yang Y, et al. The Chinese herbal formula fuzheng quxie decoction attenuates cognitive impairment and protects cerebrovascular function in SAMP8 mice. *Neuropsychiatr Dis Treat*. 2018;14:3037–3051. doi:10.2147/NDT.S175484

34. Moradi SZ, Momtaz S, Bayrami Z, Farzaei MH, Abdollahi M. Nanoformulations of herbal extracts in treatment of neurodegenerative disorders. *Front Bioeng Biotechnol*. 2020;8:238.

35. Suganthy N, Devi KP, Nabavi SF, Braidy N, Nabavi SM. Bioactive effects of quercetin in the central nervous system: focusing on the mechanisms of actions. *Biomed Pharmacother*. 2016;84:892–908. doi:10.1016/j.biopha.2016.10.011

36. Paula PC, Angelica Maria SG, Luis CH, Gloria Patricia CG. Preventive effect of quercetin in a triple transgenic alzheimer's disease mice model. *Molecules*. 2019;24(12):2287. doi:10.3390/molecules24122287

37. Zaplatic E, Bule M, Shah SZA, Uddin MS, Niaz K. Molecular mechanisms underlying protective role of quercetin in attenuating Alzheimer's disease. *Life Sci*. 2019;224:109–119. doi:10.1016/j.lfs.2019.03.055

38. Chen AY, Chen YC. A review of the dietary flavonoid, kaempferol on human health and cancer chemoprevention. *Food Chem*. 2013;138 (4):2099–2107. doi:10.1016/j.foodchem.2012.11.139

39. Tsai MS, Wang YH, Lai YY, et al. Kaempferol protects against propacetamol-induced acute liver injury through CYP2E1 inactivation, UGT1A1 activation, and attenuation of oxidative stress, inflammation and apoptosis in mice. *Toxicol Lett*. 2018;290:97–109. doi:10.1016/j.toxlet.2018.03.024

40. Yang EJ, Kim GS, Jun M, Song KS. Kaempferol attenuates the glutamate-induced oxidative stress in mouse-derived hippocampal neuronal HT22 cells. *Food Funct*. 2014;5(7):1395–1402. doi:10.1039/c4fo00068d

41. Benesch MG, McElhaney RN. A comparative calorimetric study of the effects of cholesterol and the plant sterols campesterol and brassicasterol on the thermotropic phase behavior of dipalmitoylphosphatidylcholine bilayer membranes. *Biochim Biophys Acta*. 2014;1838 (7):1941–1949. doi:10.1016/j.bbamem.2014.03.019

42. Burg VK, Grimm HS, Rothhaar TL, et al. Plant sterols the better cholesterol in Alzheimer's disease? A mechanistical study. *J Neurosci*. 2013;33(41):16072–16087. doi:10.1523/JNEUROSCI.1506-13.2013

43. Wang J, Wu F, Shi C. Substitution of membrane cholesterol with β-sitosterol promotes nonamyloidogenic cleavage of endogenous amyloid precursor protein. *Neuroscience*. 2013;247:227–233. doi:10.1016/j.neuroscience.2013.05.022

44. Ye JY, Li L, Hao QM, Qin Y, Ma CS. β-Sitosterol treatment attenuates cognitive deficits and prevents amyloid plaque deposition in amyloid protein precursor/presenilin 1 mice. *Korean J Physiol Pharmacol*. 2020;24(1):39–46. doi:10.4196/kjpp.2020.24.1.39

45. Guo LL, Guan ZZ, Huang Y, Wang YL, Shi JS. The neurotoxicity of β-amyloid peptide toward rat brain is associated with enhanced oxidative stress, inflammation and apoptosis, all of which can be attenuated by scutellarin. *Exp Toxicol Pathol*. 2013;65(5):579–584. doi:10.1016/j.etp.2012.05.003

46. Uddin MS, Kabir MT, Mamun AA, et al. Pharmacological approaches to mitigate neuroinflammation in Alzheimer's disease. *Int Immunopharmacol*. 2020;84:106479.

47. Persson T, Popescu BO, Cedazo-Minguez A. Oxidative stress in Alzheimer's disease: why did antioxidant therapy fail? *Oxid Med Cell Longev*. 2014;2014:427318. doi:10.1155/2014/427318

48. Heras-Sandoval D, Pérez-Rojas JM, Hernández-Damián J, Pedraza-Chaverri J. The role of PI3K/AKT/mTOR pathway in the modulation of autophagy and the clearance of protein aggregates in neurodegeneration. *Cell Signal*. 2014;26(12):2694–2701. doi:10.1016/j.cellsig.2014.08.019

49. Li Q, Liu Y, Sun M. Autophagy and Alzheimer's disease. *Cell Mol Neurobiol*. 2017;37(3):377–388. doi:10.1007/s10571-016-0386-8

50. Chiarini A, Dal Pra I, Marconi M, Chakravarthy B, Whitfield JF, Armato U. Calcium-sensing receptor (CaSR) in human brain's pathophysiology: roles in late-onset Alzheimer's disease (LOAD). *Curr Pharm Biotechnol*. 2009;10(3):317–326. doi:10.2174/138920109787847501

51. Puig B, Gómez-Isla T, Ribé E, et al. Expression of stress-activated kinases c-Jun N-terminal kinase (SAPK/JNK-P) and p38 kinase (p38-P), and tau hyperphosphorylation in neurites surrounding betaA plaques in APP Tg2576 mice. *Neuropathol Appl Neurobiol*. 2004;30(5):491–502. doi:10.1111/j.1365-2990.2004.00569.x

52. Marques CA, Keil U, Bonert A, et al. Neurotoxic mechanisms caused by the Alzheimer's disease-linked Swedish amyloid precursor protein mutation: oxidative stress, caspases, and the JNK pathway. *J Biol Chem*. 2003;278(30):28294–28302. doi:10.1074/jbc.M212265200

53. Hashimoto Y, Tsuji O, Niikura T, et al. Involvement of c-Jun N-terminal kinase in amyloid precursor protein-mediated neuronal cell death. *J Neurochem*. 2003;84(4):864–877. doi:10.1046/j.1471-4159.2003.01585.x

54. Tamagno E, Parola M, Bardini P, et al. Beta-site APP cleaving enzyme up-regulation induced by 4-hydroxynonenal is mediated by stress-activated protein kinases pathways. *J Neurochem*. 2005;92 (3):628–636. doi:10.1111/j.1471-4159.2004.02895.x

55. Shen C, Chen Y, Liu H, et al. Hydrogen peroxide promotes Abeta production through JNK-dependent activation of gamma-secretase. *J Biol Chem*. 2008;283(25):17721–17730. doi:10.1074/jbc.M800013200

56. Schnöder L, Hao W, Qin Y, et al. Deficiency of neuronal p38α MAPK attenuates amyloid pathology in Alzheimer disease mouse and cell models through facilitating lysosomal degradation of BACE1. *J Biol Chem*. 2016;291(5):2067–2079. doi:10.1074/jbc.M115.695916

57. Layfield R, Cavey JR, Lowe J. Role of ubiquitin-mediated proteolysis in the pathogenesis of neurodegenerative disorders. *Ageing Res Rev.* 2003;2(4):343–356. doi:10.1016/S1568-1637(03)00025-4

58. Hegde AN, Smith SG, Duke LM, Pourquoi A, Vaz S. Perturbations of ubiquitin-proteasome-mediated proteolysis in aging and Alzheimer's disease. *Front Aging Neurosci.* 2019;11:324. doi:10.3389/fnagi.2019.00324

59. Chu J, Li JG, Hoffman NE, Madesh M, Praticò D. Degradation of gamma secretase activating protein by the ubiquitin-proteasome pathway. *J Neurochem.* 2015;133(3):432–439. doi:10.1111/jnc.13011

60. Hong L, Huang HC, Jiang ZF. Relationship between amyloid-beta and the ubiquitin-proteasome system in Alzheimer's disease. *Neurol Res.* 2014;36(3):276–282. doi:10.1179/1743132813Y.0000000288

61. Gong B, Radulovic M, Figueiredo-Pereira ME, Cardozo C. The ubiquitin-proteasome system: potential therapeutic targets for Alzheimer's disease and spinal cord injury. *Front Mol Neurosci.* 2016;9:4. doi:10.3389/fnmol.2016.00004

62. Thiel G, Rössler OG. Resveratrol stimulates AP-1-regulated gene transcription. *Mol Nutr Food Res.* 2014;58(7):1402–1413. doi:10.1002/mnfr.201300913

63. Meng J, Li Y, Zhang M, et al. A combination of curcumin, vorinostat and silibinin reverses Aβ-induced nerve cell toxicity via activation of AKT-MDM2-p53 pathway. *PeerJ.* 2019;7:e6716. doi:10.7717/peerj.6716